Impact of visible light illumination on ultraviolet emission from ZnO nanocrystals

S. S. Kurbanov,[1,2,*] G. N. Panin,[1,3] T. W. Kim,[4] and T. W. Kang[1]
[1]*Quantum-Functional Semiconductor Research Center, Dongguk University, Seoul 100715, Republic of Korea*
[2]*Heat Physics Department, Uzbekistan Academy of Sciences, Tashkent 700135, Uzbekistan*
[3]*IMT&HPM, RAS, Chernogolovka, Moscow distr. 142432, Russia*
[4]*Advanced Semiconductor Research Center, Division of Electronics and Computer Engineering, Hanyang University, Seoul 133791, Republic of Korea*
(Received 2 April 2008; revised manuscript received 5 June 2008; published 14 July 2008)

The influence of a visible Ar^+-laser (488 nm) illumination on photoluminescence (PL) from ZnO nanocrystals excited by He-Cd laser (325 nm) at various excitation intensities and temperatures was investigated. A reversible quenching of the UV near-band-edge emission under Ar^+-laser illumination was observed. The quenching effect increases with decreasing temperature and He-Cd laser intensity at fixed intensity of Ar^+-laser. It is found that the recovery time of the initial PL intensity depends on temperature and Ar^+-laser exposure time. At room temperature the PL restored the initial intensity instantly after the turning off the Ar^+-laser illumination; however at 10 K this process took several minutes. The proposed mechanism of the observed quenching effect implies an appearance of the additional recombination channel under a visible light illumination due to the recharging of oxygen-vacancy states in the surface depletion zone.

DOI: 10.1103/PhysRevB.78.045311 PACS number(s): 78.55.Et, 61.80.Ba

I. INTRODUCTION

Zinc oxide (ZnO) is a II-VI compound semiconductor with a wide direct band gap of 3.37 eV at room temperature (RT), which makes it interesting for optoelectronic devices in the near UV region.[1–3] ZnO has a large exciton binding energy of about 60 meV, which promises efficient RT exciton emission. The RT photoluminescence (PL) spectrum of ZnO along with the exciton emission band at near 380 nm contains a deep-level defect related emission band at 500–650 nm. The deep-level emission band, as usual, is considered consisting of the green (500–520 nm), yellow-orange (560–600 nm), and red (650 nm) bands. The green emission band is frequently observed and the early studies it was attributed to copper impurities.[3] However at present, oxygen vacancies have been assumed to be the most likely candidate for recombination centers involved in the green luminescence of ZnO.[4–9] UV (exciton) and visible (defect) emissions are in competition with each other and it is presumed that the deep-level emission centers are preferable channels of the electron-hole recombination. Such behavior of the PL bands gives rise to interesting physical phenomena, which creates an ability to control the intensity of the UV emission, and could be also of practical relevance. In practice the dependence of the excitonic band on external and internal perturbations is widely used to modulate its intensity. The modulations of the excitonic PL by means of acoustic[10] and terahertz waves[11] as well as the excitonic PL and CL by electrical field[12,13] were reported. The opportunity to control the characteristics, in particular, reflectance, of the sample under study by the external periodic perturbations serves as a basis for the modulation spectroscopy and allow us to study electron states and features of the semiconductor band structure.[14–16] In ZnO nanocrystals the electron-paramagnetic-resonance signal assigned to singly ionized oxygen vacancy (V_O^+) was observed to be photosensitive for photon energies down to as low as 2.3 eV.[4,5] Upon illumination, the V_O^+ density was observed to grow. Moreover, it has been found that the intensity of the green emission in ZnO powder correlates well with the paramagnetic single-ionized oxygen-vacancy (V_O^+) density. Nevertheless, the effect of the subband illumination on emission from ZnO is still unclear and remains unexplored in spite of the observed correlation between the density of V_O^+ and the green emission intensity and the sensitivity of V_O^+ to a visible light.

In this work we have undertaken a study of the visible light illumination effect on near-band-edge emission intensity from ZnO nanocrystals excited by UV He-Cd laser radiation (325 nm). It is found that a cw Ar^+-laser irradiation (488 nm) in addition to the UV excitation can effectively (up to 75%) reduce the exciton emission from ZnO. This reduction in integrated intensity $\Delta I/I$ (hereafter called quenching) of the near-band-edge emission is reversible and has a pronounced dependence on temperature and ratio of Ar^+ and He-Cd laser power densities. We identify the observed UV emission quenching effect as being due to the light induced recharging of oxygen-vacancy states in the surface depletion zone of ZnO nanocrystals.

II. EXPERIMENTAL

PL studies were carried out on a SPEX spectrometer equipped with a 0.75 m grating monochromator using a 50 mW cw He-Cd laser operating at the wavelength of 325 nm as the excitation source. At the exit slit of the monochromator a cooled photomultiplier tube (Hamamatsu R943-02) was mounted. PL spectra were measured in the backscattering configuration and the registration of the PL signal was carried out by using a conventional lock-in technique with a mechanical chopper. A 12 mW cw Ar^+-laser operating at the wavelength of 488 nm (2.54 eV) was used as an additional illumination source. Both the laser beams were focused on the sample by employing quartz lenses. The beam spot size after the lens was estimated to be about 100 μm in diameter

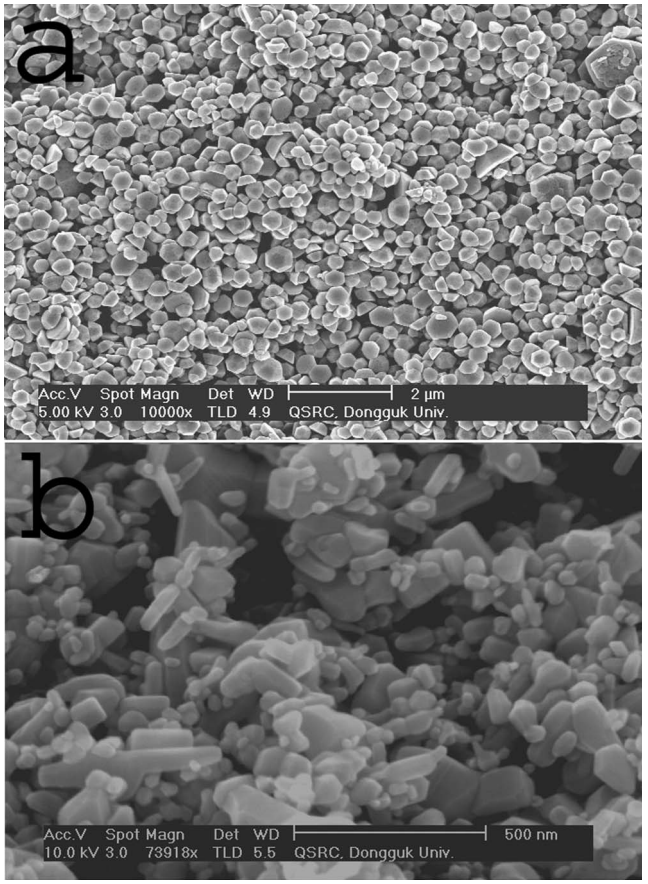

FIG. 1. SEM images of (a) CSD ZnO nanocrystals and (b) ZnO powder.

and the Ar^+-laser beam's spot covered the He-Cd-laser's spot. In order to vary the excitation intensity (power density), the spot size was kept constant while the input power was attenuated by the neutral filters. The corresponding maximum intensities of laser beams at 325 and 488 nm were estimated to be about 500 and 120 W/cm^2, respectively. The samples were mounted on the cold finger of a closed-cycle helium cryostat and the sample temperature was controlled in the range from 10 K up to room temperature.

Three types of ZnO samples were prepared for the study: (1) ZnO nanocrystals deposited on a sapphire substrate by a chemical solution deposition (CSD) method as reported previously[17,18] and annealed in air at 500 °C for 1 h, (2) ZnO powder (Aldrich), and (3) ZnO film grown on a sapphire substrate by using the molecular-beam epitaxy method. Morphologies of samples were investigated by using a high-resolution scanning electron microscope (SEM) (XL-30 PHILIPS). Figure 1 shows the SEM images of (a) CSD ZnO nanocrystals and (b) ZnO powder. The CSD nanocrystals have the regular cone form and the size of 100–500 nm. ZnO powder consists of 10–100 nm size nanoparticles.

III. RESULTS

Figure 2 shows the typical RT PL spectra of ZnO samples: (a) powder, (b) CSD nanocrystals, and (c) film excited by

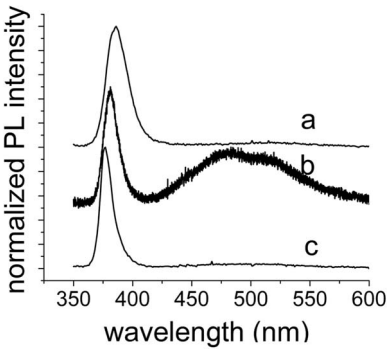

FIG. 2. RT PL spectra from ZnO (a) powder, (b) nanocrystals, and (c) films excited by He-Cd laser radiation (power density of ~50 W/cm^2). Spectra have been normalized to their maxima and the curves are vertically arbitrarily shifted for a better comparison.

He-Cd laser radiation at moderate (50 W/cm^2) power density. All spectra display the dominant near-band-edge emission peak in the UV region (377–386 nm) and a broad visible emission band around 500 nm. ZnO nanocrystals prepared by the CSD method manifest higher visible emission intensity than other samples. The UV PL bands are attributed to free exciton emissions while the visible emission band is related to oxygen-vacancy center. Illumination of the samples with a cw Ar^+-laser radiation, in addition to the He-Cd laser excitation, results in a decrease in intensity of the UV PL band while the visible emission intensity slightly increases. It should be noted that under the single 488 nm illumination, no luminescence from ZnO nanocrystals was observed. The quenching effect has been observed in all samples investigated; however it was more pronounced in CSD ZnO nanocrystals. Taking into account this circumstance we present the results related to the CSD ZnO nanocrystals.

Figures 3(a) and 3(b) display the RT PL spectra collected from CSD ZnO nanocrystals under single (He-Cd laser) (black) and double (He-Cd and Ar^+-lasers) (red) illuminations at different excitation power densities of He-Cd laser. The quenching effect depends strongly on the power-density ratio of the employed lasers (I_{488}/I_{325})—with increasing the I_{488}/I_{325} ratio the magnitude of the quenching increases. An increase in power density of the He-Cd laser by 2 orders of magnitude, at the constant Ar^+-laser intensity of 120 W/cm^2, results in an increase in the integrated intensity quenching ($\Delta I/I$) of the UV emission from 0.07 (7%) to 0.14 (14%). The observed quenching effect is reversible; the PL restores the initial intensity and form instantly after the turning off the Ar^+-laser illumination regardless of excitation power density.

Variations of He-Cd laser power density have been found to affect also a position of the UV peak. With increasing the excitation power density the UV peak shifts toward higher wavelength (from 382 to 385 nm). This redshift of the UV emission peak could be originated from the ZnO band-gap shrinkage due to laser heating of nanocrystals.[18–21]

Figures 4(a) and 4(b) show the PL spectra of ZnO nanocrystals recorded at different (50 and 0.50 W/cm^2) excitation power densities of He-Cd laser at 10 K. The spectra

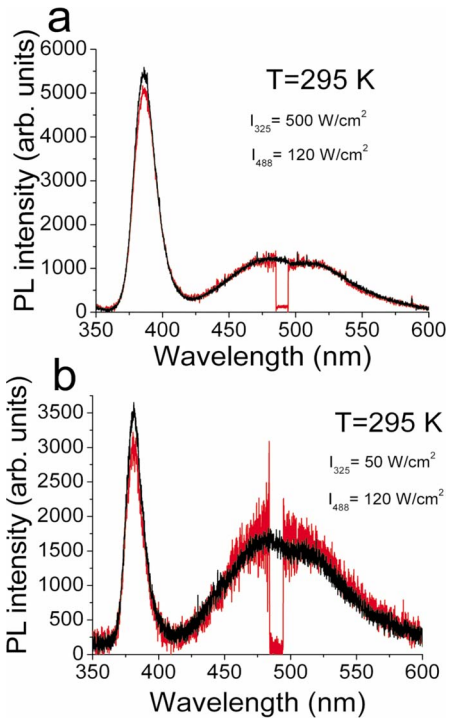

FIG. 3. (Color online) RT PL spectra collected from CSD ZnO nanocrystals under single (He-Cd laser) (black) and double (He-Cd and Ar^+-lasers) (red) laser illuminations at different excitation power densities of He-Cd laser: (a) $I_{325} \sim 500$ W/cm^2 and $I_{488} \sim 120$ W/cm^2 and (b) $I_{325} \sim 50$ W/cm^2 and $I_{488} \sim 120$ W/cm^2. (To protect the photomultiplier tube from the scattered Ar^+-laser radiation around 488 nm the spectrometer's slit was shut down.)

obtained at the 50 W/cm^2 power densities exhibit a dominant near-band-edge emission peak at 368.6 nm and two emission bands at 373.6 and 382.8 nm as well as a relatively weak visible emission peak at around 500 nm. Peak at 368.6 nm is attributed to the emission of donor bound exciton.[1–3] The other emission bands could be ascribed to donor-acceptor-pair recombination[22] or exciton phonon replicas[23] or two photon transitions.[24]

The UV emission quenching effect was found to depend strongly on temperature. With the decrease in temperature to 10 K the magnitude of the quenching increases and under the He-Cd laser power density of 50 W/cm^2, it reaches to 0.38 (38%) [Fig. 4(a)]. The reducing of the He-Cd laser power density by 2 orders of magnitude at the fixed Ar^+-laser power density increases the quenching value up to 0.55 (55%) [Fig. 4(b)].

It is obviously that the quenching effect strongly depends on the power-density ratio of Ar^+ and He-Cd lasers. The highest effect achieved in our experiments was ~75%. It was obtained at 10 K when the power-density ratio of the Ar^+ and He-Cd lasers was 500 (Fig. 5). The reversible behavior of the quenching effect remains also at low temperatures. However the time required reestablishing the initial PL intensity increases with a decrease in temperature. At 10 K the recovery time takes several minutes. Moreover the recovery time was found to depend on an illumination time by Ar^+-laser. The long term illumination results in prolongation of the recovery time of the PL intensity. The restoration of the PL initial intensity could be significantly accelerated by using a short-term increasing of temperature.

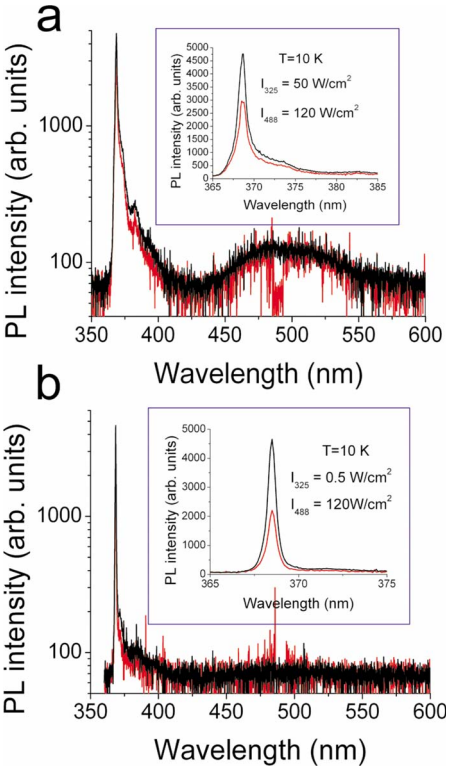

FIG. 4. (Color online) PL spectra collected from CSD ZnO nanocrystals under single (He-Cd laser) (black) and double (He-Cd and Ar^+-lasers) (red) laser illuminations at different excitation power densities of He-Cd laser at 10 K: (a) $I_{325} \sim 50$ W/cm^2 and $I_{488} \sim 120$ W/cm^2 and (b) $I_{325} \sim 0.50$ W/cm^2 and $I_{488} \sim 120$ W/cm^2. The inset shows the details of spectra in the region of 365—385 nm. (To protect the photomultiplier tube from the scattered Ar^+-laser radiation around 488 nm the spectrometer's slit was shut down.)

IV. DISCUSSION

The obtained results indicate that the additional Ar^+-laser illumination of ZnO nanocrystals creates a new partway for

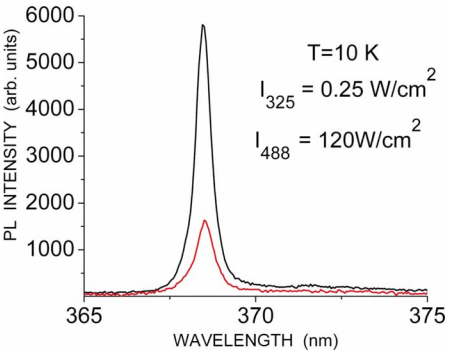

FIG. 5. (Color online) PL spectra collected from CSD ZnO nanocrystals under single (He-Cd laser) (black) and double (He-Cd and Ar^+-lasers) (red) laser illuminations at different excitation power densities of He-Cd laser at 10 K: $I_{325} \sim 0.25$ W/cm^2 and $I_{488} \sim 120$ W/cm^2.

excited charge-carrier recombination, which results in quenching of the near-band-edge emission intensity. Obviously, the energy of Ar^+-laser radiation (2.54 eV) is not enough to create new defects in ZnO lattice. However such low-energy photons can effect on charge states of the existing defects. As was identified in previous studies, the major defect related PL band at around 500 nm is originated from oxygen-vacancy center and the quenching effect also was more pronounced in samples with higher relative intensity of this band. Therefore oxygen vacancies first of all should be considered as centers responsible for the visible light induced quenching effect. Oxygen vacancies in ZnO can occur in three different charge states: the V_O^0 state which has captured two electrons and is neutral relative to the lattice, the singly ionized V_O^+ state with one electron, and the V_O^{++} state which has no electrons and is doubly positively charged with respect to the lattice. Only the V_O^+ state is paramagnetic and consequently observable by EPR measurements. It is well known that the ZnO particle surface layer contains an electron depletion region created due to the surface states. The existence of such region results in the band bending at the surface. In the fraction of the depletion region where the Fermi level passes below the V_O^+/V_O^{++} energy level, all oxygen vacancies will be in the diamagnetic V_O^{++} state while oxygen vacancies in V_O^+ state will exist in the particle core. The first principle studies have shown[25–28] that the oxygen vacancy is a "negative-*U*" center, i.e., V_O^+ state is deeper (farther from the conduction band) than either V_O^{++} or V_O^0 for any Fermi-level position. As already mentioned the intensity of the green luminescence in ZnO correlates very well with the paramagnetic single-ionized oxygen-vacancy density.[4,5] V_O^+ is found to be photosensitive for photons with an energy of >2 eV and this effect was explained by converting some of the V_O^{++} centers to the paramagnetic V_O^+ state. Considering these results and fact that the photon energy of Ar^+-laser radiation is 2.54 eV, the observed quenching effect of the near-band-edge emission from ZnO nanocrystals is well interpreted in terms of recharging of the oxygen-vacancy centers.

Since V_O^{++} centers can be easily formed in the depletion region, consequently their number depends on the depletion region width. The width of a depletion region (W) is given by

$$W = (2\varepsilon_{\mathrm{ZnO}} V_{\mathrm{bi}}/eN_D)^{1/2}, \tag{1}$$

where V_{bi} is the potential at the surface, e is the electron charge, N_D is the donor density, and $\varepsilon_{\mathrm{ZnO}}$ is the static dielectric constant of ZnO.[29] As can be seen from Eq. (1), the width of the depletion region is inversely proportional to the square root of the free-carrier concentration in the nanocrystal and proportional to the potential at the surface. It is well known that in the case of high excitation, the surface potential depends on excitation intensity.[29] At high intensities the width of the depletion region is smaller than at low intensities owing to the reduced surface potential. On the other hand an increase in temperature leads to additional narrowing of the depletion region due to the increase in the free-carrier concentration. The simultaneous action of these factors (i.e., the increase in excitation intensity and temperature) results in the strong decrease in the depletion region width, consequently, the concentration of V_O^{++} centers. These speculations are in the good agreement with a strong increase in the quenching effect with a decrease in excitation power density and temperature. The temperature lowering from 295 to 10 K and a decrease in excitation intensity in 3 orders of magnitude (from 500 to 0.5 $\mathrm{W/cm^2}$) resulted in a large enhancement of the quenching effect (from 7% up to 53%) at the fixed Ar^+-laser power density of 120 $\mathrm{W/cm^2}$.

Even though the Ar^+-laser illumination quenches well the UV emission, its impact on the visible emission intensity is observed very week. Although at room temperature under the double illumination the visible emission intensity slightly increases, at low temperatures it is rather unremarkable. This circumstance may be originated from different excitation efficiencies of the UV and visible emissions depending on temperature and excitation power density. One can see a decrease in temperature results in an increase in ratio of intensity of the UV emission to that of the visible emission. It increases from $\sim$2.25 to $\sim$66.5 with the decrease in temperature from 295 to 10 K at low excitation power density. Such behavior indicates that at low temperatures the visible emission is excited with relatively low efficiency than UV emission and the effect of Ar^+-laser irradiation on the visible PL, probably, also decreases. On the other hand, Ar^+-laser illumination could induce mostly the nonradiative states. It is known that there exists another type of single-ionized oxygen-vacancy-related center: V_O^+ complex,[30] which can be formed in the presence of nearby interstitial oxygen (Frenkel pair).[31] This center unlike the isolated V_O^+ is not a green luminescent site, even though it shows a somewhat similar nature. Moreover the V_O^+ complex may act as a quenching center for radiative recombination in ZnO. The CSD technique used to grow ZnO nanocrystals provides the oxygen rich samples.[18] This circumstance allows us to infer that in the ZnO nanocrystals prepared in the oxygen rich conditions, some of V_O^{++} centers under Ar^+-laser illumination creates V_O^+-complex which does not take part in green emission but acts as nonradiative, quenching center for UV PL.

The reversible behavior of the quenching effect and dependence of the recovery time on temperature and exposure time by the visible light confirm the proposed recharging model of the oxygen-vacancy-related centers in the ZnO nanocrystal depletion region. As was reported,[4] the EPR signal from V_O^+ decays when illumination was interrupted and at 294 K this decay is instantaneous, but at 150 K it requires several minutes. In our experiments the recovery process of the UV emission intensity could be also accelerated by a short-term rising of temperature. These observations indicate that there is some energetic barrier, escaping of which the system can return into the initial state. The existence of energetic barrier for decay of photogenerated V_O^+ into the other charge states was predicted by Walle[26] based on the first-principles investigation.

The observed quenching of the UV emission could be caused also by the heating of ZnO nanocrystals induced by the additional Ar^+-laser illumination. In order to examine this effect the temperature dependent PL spectra of the ZnO nanocrystals have been investigated (Fig. 6). The spectra show a typical for ZnO nanocrystals temperature

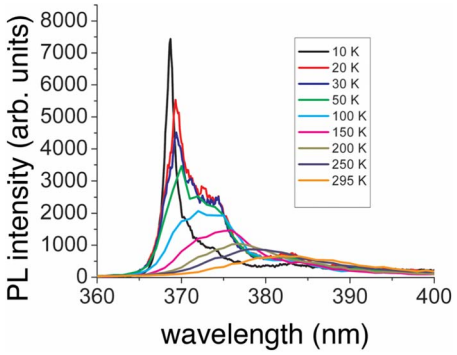

FIG. 6. (Color online) Temperature dependent PL spectra of the ZnO nanocrystals.

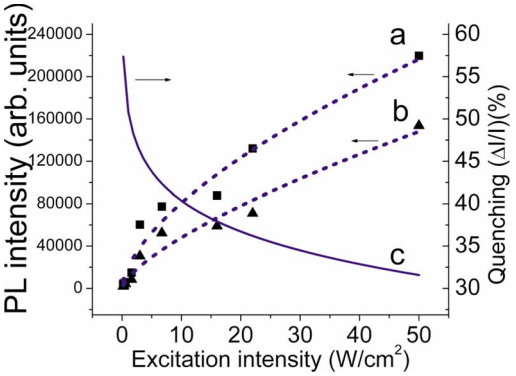

FIG. 7. (Color online) Integrated exciton PL intensity (a) without and (b) under Ar^+-laser illumination as well as (c) the quenching of the PL intensity as a function of He-Cd laser excitation power density at 10 K. The dash lines are the fit to a power law (see the text).

dependence—with increasing temperature the PL intensity decreases and redshift of the exciton peak position occurs. With increasing the sample temperature from 10 to 20 K the PL intensity deceased to approximately 25% and the donor bound exciton peak shifted from 368.6 to 369.3 nm. Thus, an increase in temperature led at once to decrease in the PL intensity and redshift of the exciton emission peak due to band-gap shrinkage. However, in opposite to temperature effect, the additional Ar^+-laser illumination affects only the PL intensity and does not change the exciton emission-peak position. This finding undoubtedly indicated that the quenching effect is not induced by Ar^+-laser heating.

For a further understanding of the mechanism of the observed UV PL band quenching, we investigated the quenching effect dependence on the excitation power density in details. The integrated PL intensity versus the excitation power density under (a) the single (He-Cd laser) and (b) the double (He-Cd-and Ar^+-lasers) illuminations as well as (c) the quenching $(\Delta I/I)$ of the UV emission at 10 K are plotted in Fig. 6. The both PL intensity dependences display a tendency to saturation at high excitation level. The luminescence intensity I versus excitation power density can be expressed as

$$I = \eta I_0^{\alpha}. \tag{2}$$

In this relation I_0 is the power density of the excitation laser radiation, η is the constant of proportionality (some authors define it as an emission efficiency), and the exponent α represents the radiative recombination mechanism. For excitonic recombination, $1<\alpha<2$, for band-gap emission, i.e., electron-hole bimolecular recombination, $\alpha \sim 2$, and α is less than 1 when an impurity is involved in the transitions, as well as for donor-acceptor transitions.[32,33] Using Eq. (2) to fit the data of the single and double laser illuminations we found $\alpha \sim 0.61$ and $\alpha \sim 0.7$, respectively. The obtained values of the exponent α are less 1 and they could be interpreted as evidence that the UV emission originates from native donor-acceptor transitions or impurities. However all results undoubtedly indicate that UV PL has exciton nature. As is well known, a saturation effect of the excitonic emission under high-power excitation is not rarely observed phenomenon.[32,33] The saturation of the excitonic emission from GaN powder excited in ambient air at RT was ascribed to a thermally activated nonradiative process due to laser heating of particles.[32] A slow increase and saturation of the PL intensity of free excitons in a GaInAsSb/GaAlAsSb single-quantum-well structure under higher excitation intensity observed at 10 K was attributed to the exciton screening effect.[33] It seems in our experiment that both suggested saturation mechanisms are present. The ZnO nanocrystals deposited on a sapphire substrate create several quasi-isolated layers and at the same time, the high-power-density excitation of the nanocrystals occurs at low (10 K) temperature. As observed in Fig. 1(a) the ZnO nanocrystals are not well packed and the laser-induced heat transfer can take place from the upper layer of the nanocrystals to the lower layers only via the particles which are in contact with each other. Since cooling of the nanocrystals occurs by way of a substrate and the lower layers, under such conditions the top layer can have significant higher temperature then the layers located close to the substrate due to their low thermal conductivity.

The visible light illumination increases the exponent α from 0.61 to 0.70 by of approximately 15%. This growth undoubtedly is not result of a decrease in the laser heating. It originates rather from a decrease in exciton relative population due to opening an additional channel of recombination. Although this channel is basically nonradiative, the decrease in exciton relative population can reduce the exciton screening effect and provide a faster increase in the PL intensity with excitation power than that in the case of the single He-Cd laser illumination. The saturation of the UV PL intensity at high excitation power densities also appears in the quenching effect. In the present experiment with increasing the He-Cd laser power density from 0.14 to 50 W/cm^2 the quenching decreases from 58% up to 32% (Fig. 7). Obliviously, reduction in the quenching effect results basically from the change of intensity ratio of Ar^+ and He-Cd lasers (I_{488}/I_{325}), but the loss of linearity in this dependence is caused by the saturation behavior of the UV PL intensity at high excitation power densities.

It may be expected that use of the observed quenching effect allows effectively modulate the UV emission from ZnO and an employment of high power lasers with wavelength in the 450–550 nm region could provide it. In this

context the quenching effect may find application in ZnO based optoelectronic devices and optical communication systems.

V. CONCLUSION

The impact of visible Ar^+-laser illumination (488 nm) on the UV emission from ZnO nanocrystals excited by He-Cd laser (325 nm) at various excitation intensities and temperatures has been investigated. It was found that a visible light illumination simultaneously with UV excitation results in a decrease in the near-band-edge emission intensity. The quenching effect depends on the intensity ratio of the visible and UV lasers, temperature, and the relative intensity of the green PL band. The highest quenching effect (75%) was achieved at $I_{488}/I_{325} \sim 500$ at 10 K. The quenching of the UV emission is reversible and the recovery time depends on temperature and exposure time of Ar^+-laser radiation. While at room temperature the restoration of the initial intensity of the UV emission after stopping the Ar^+-laser illumination occurred instantaneously, at 10 K this process required several minutes. The quenching effect of the UV emission observed in ZnO samples is suggested to be due to the recharging of oxygen-vacancy states in the surface depletion zone under a visible light irradiation.

ACKNOWLEDGMENTS

The authors would like to thank Sh. U. Yuldashev for helpful discussions. This work was supported in part by funds of the Quantum-functional Semiconductor Research Center and Dongguk University and by the Korea Science and Engineering Foundation (KOSEF) grant funded by the Korea government (MOST) (Grant No. R0A-2007-000-20044-0).

*Corresponding author; saidislam_kurbanov@yahoo.com

[1] D. C. Look, Mater. Sci. Eng., B **80**, 383 (2001).
[2] T. W. Kang, Sh. Yuldashev, and G. N. Panin, in *Handbook of Semiconductor Nanostructures and Nanodevices*, edited by A. A. Balandin and K. L. Wang (American Scientific, Los Angeles, 2005).
[3] Ü. Özgür, Ya. I. Alivov, C. Liu, A. Teke, M. A. Reshchikov, S. Doğan, V. Avrutin, S.-J. Cho, and H. Morkoç, J. Appl. Phys. **98**, 041301 (2005).
[4] K. Vanheusden, C. H. Seager, W. L. Warren, D. R. Tallant, and J. A. Voigt, Appl. Phys. Lett. **68**, 403 (1996).
[5] K. Vanheusden, W. L. Warren, C. H. Seager, D. R. Tallant, and J. A. Voigt, J. Appl. Phys. **79**, 7983 (1996).
[6] S. A. Studenikin, N. Golego, and M. Cocivera, J. Appl. Phys. **84**, 2287 (1998).
[7] A. van Dijken, E. A. Meulenkamp, D. Vanmaekelbergh, and A. Meijerink, J. Lumin. **87-89**, 454 (2000).
[8] F. H. Leiter, H. R. Alves, A. Hofstaetter, D. M. Hofmann, and B. K. Meyer, Phys. Status Solidi B **226**, R4 (2001).
[9] W. Cheng, P. Wu, X. Zou, and T. Xiao, J. Appl. Phys. **100**, 054311 (2006).
[10] Y. Takagaki, E. Wiebicke, A. Riedel, M. Ramsteiner, H. Kostial, R. Hey, and K. H. Ploog, Semicond. Sci. Technol. **18**, 807 (2003).
[11] M. A. J. Klik, T. Gregorkiewicz, I. N. Yassievich, V. Yu. Ivanov, and M. Godlewski, Phys. Rev. B **72**, 125205 (2005).
[12] S. K. Zhang, P. V. Santos, and R. Hey, Appl. Phys. Lett. **78**, 1559 (2001).
[13] G. N. Panin, T. W. Kang, A. N. Aleshin, A. N. Baranov, Y.-J. Oh, and I. A. Khotina, Appl. Phys. Lett. **86**, 113114 (2005).
[14] L. Aigouy, T. Holden, F. H. Pollak, N. N. Ledentsov, W. M. Ustinov, P. S. Kopev, and D. Bimberg, Appl. Phys. Lett. **70**, 3329 (1997).
[15] G. L. Rowland, T. J. C. Hosea, S. Malik, D. Childs, and R. Murray, Appl. Phys. Lett. **73**, 3268 (1998).
[16] M. Motyka, G. Sek, R. Kudrawiec, J. Misiewicz, L. H. Li, and A. Fiore, J. Appl. Phys. **100**, 073502 (2006).
[17] H. Wang, Ch. Xie, and D. Zeng, J. Cryst. Growth **277**, 372 (2005).
[18] S. Kurbanov, G. Panin, T. W. Kim, and T. W. Kang, Jpn. J. Appl. Phys., Part 1 **46**, 4172 (2007).
[19] K. A. Alim, V. A. Fonoberov, M. Shamsa, and A. A. Balandin, J. Appl. Phys. **97**, 124313 (2005).
[20] K. A. Alim, V. A. Fonoberov, and A. A. Balandin, Appl. Phys. Lett. **86**, 053103 (2005).
[21] Y. Yang, H. Yan, Z. Fu, B. Yang, L. Xia, Y. Xu, J. Zuo, and F. Li, J. Phys. Chem. B **110**, 846 (2006).
[22] E. Tomzig and R. Helbig, J. Lumin. **14**, 403 (1976).
[23] D. C. Reynolds and T. C. Collins, Phys. Rev. **185**, 1099 (1969).
[24] S A. Studenikin, Michael Cocivera, W. Kellner, and H. Pascher, J. Lumin. **91**, 223 (2000).
[25] A. F. Kohan, G. Ceder, D. Morgan, and Chris G. Van de Walle, Phys. Rev. B **61**, 15019 (2000).
[26] C. G. Van de Walle, Physica B (Amsterdam) **308-310**, 899 (2001).
[27] S. B. Zhang, S.-H. Wei, and A. Zunger, Phys. Rev. B **63**, 075205 (2001).
[28] S. Lany and A. Zunger, Phys. Rev. B **72**, 035215 (2005).
[29] S. A. Studenikin, N. Golego, and M. Cocivera, J. Appl. Phys. **83**, 2104 (1998).
[30] K. Vanheusden, C. H. Seager, W. L. Warren, D. R. Tallant, J. Caruso, M. J. Hampden-Smith, and T. T. Kodas, J. Lumin. **75**, 11 (1997).
[31] K. Hoffmann and D. Hahn, Phys. Status Solidi A **24**, 637 (1974).
[32] L. Bergman, X. B. Chen, J. L. Morrison, J. Huso, and A. P. Purdy, J. Appl. Phys. **96**, 675 (2004).
[33] Sh. Jin, Y. Zheng, and A. Li, J. Appl. Phys. **82**, 3870 (1997).